



**Precision Measurements of $F_2(x, Q^2)$ and $xF_3(x, Q^2)$ by the CCFR
Collaboration Using ν_μ Scattering at the Tevatron**

P.Z.Quintas, W.C.Leung, S.R.Mishra, C.Arroyo, K.T.Bachmann *, R.E.Blair †,
C.Foudas ‡, B.J.King, W.C.Lefmann, E.Oltman §, S.A.Rabinowitz, F.J.Sciulli,
W.G.Seligman, M.H.Shaevitz
Columbia University, New York, NY 10027

F.S.Merritt, M.J.Oreglia, B.A.Schumm§
University of Chicago, Chicago, IL 60637

R.H.Bernstein, F. Borcharding, H.E.Fisk, M.J.Lamm, W.Marsh, K.W.B.Merritt,
H.Schellman, D.D.Yovanovitch
Fermilab, Batavia, IL 60510

A.Bodek, H.S.Budd, P. de Barbaro, W.K.Sakumoto
University of Rochester, Rochester, NY 14627

W.H. Smith, P.H. Sandler
University of Wisconsin, Madison, WI. 53706

Talk Presented by M.H.Shaevitz
at the Particles and Fields '91 Conference
Vancouver, Canada , Aug., 1991

ABSTRACT

We present new measurements of the nucleon structure functions $F_2(x, Q^2)$ and $xF_3(x, Q^2)$ derived from $\nu_\mu(\bar{\nu}_\mu)$ charged current interactions. The results were taken from a sample of 1,281,000 ν_μ and 270,000 $\bar{\nu}_\mu$ events obtained in two runs of the Fermilab Tevatron Quad-Triplet Beam using the Lab E neutrino detector. The data show for the first time a Q^2 evolution of xF_3 consistent with that expected from QCD. Comparisons of $F_2(x, Q^2)$ and $xF_3(x, Q^2)$ with other measurements show good agreement with the SLAC eD and BCDMS μ D data but differ from the CDHSW ν Fe and EMC μ Fe data.

*Present address: Widener Univ., Chester, PA 19013.

†Present address: Argonne National Laboratory, Argonne, IL, 60439.

‡Present address: Univ. of Wisconsin, Madison, WI, 53706.

§Present address: LBL, Berkeley, CA 94720.

1. Introduction

Neutrino scattering provides a unique technique for measuring both the $F_2(x, Q^2)$ and $xF_3(x, Q^2)$ structure functions which are associated, in the quark parton model, with the total quark ($q + \bar{q}$) and valence quark ($q - \bar{q}$) momentum, respectively. The predicted Q^2 evolution of xF_3 is particularly simple since it is not coupled to the unknown gluon distribution and, therefore, can be used as a unambiguous test of perturbative Quantum Chromodynamics and measurement of $\Lambda_{\overline{MS}}$. Combined analyses of F_2 and xF_3 allow the separation of the gluon evolution component and lead to information on the gluon structure function.

The differential cross-section for charged current interactions is given by:

$$\frac{d^2\sigma^{\nu(\bar{\nu})}}{dx dy} = \frac{G^2 s}{2\pi} \left[\left(1 - y - \frac{Mxy}{2E}\right) F_2(x, Q^2) + \frac{y^2}{2} 2xF_1(x, Q^2) \pm y\left(1 - \frac{y}{2}\right) xF_3(x, Q^2) \right]$$

We extract the structure functions from the measured number of $\nu_\mu(\bar{\nu}_\mu)$ events and incident neutrino flux. The key items necessary for a precision measurement are 1) an accurately measured $\nu_\mu(\bar{\nu}_\mu)$ flux, 2) well understood experimental resolutions on the measured event parameters (P_μ , θ_μ , and E_{HAD}), 3) a well determined absolute energy scale for both the P_μ and E_{HAD} measurements, and 4) high statistics over a broad energy range.

The preliminary results reported here are from data taken in two runs in the Fermilab Tevatron Quad-Triplet beam with neutrino energies up to 600 GeV. A sample of 3,700,00 triggers was reduced after fiducial and kinematic cuts ($P_\mu > 15$ GeV, $\theta_\mu < .150$, and $E_{HAD} > 10$ GeV) to 1,281,000 ν_μ - and 270,000 $\bar{\nu}_\mu$ -induced events.

2. Detector Calibration and Flux Determination

The CCFR Lab E neutrino detector consists of a target calorimeter with iron plates, scintillation counters, and drift chambers followed by a solid iron toroid muon spectrometer. The detector was calibrated using charged particle test beams directed into the apparatus. For the hadron energy calibration,¹ a hadron beam was directed into the target at various energies and positions. Each beam particle was momentum analyzed to better than one percent leading to a resolution function known over three decades and an absolute calibration known to $\approx .8\%$. Test beam muons were used to calibrate the toroid spectrometer² giving an absolute calibration known to better than .6%. The resolution function is dominated by energy loss mechanisms in the iron toroid, which were simulated using Monte Carlo techniques and found to agree with the test beam results over three decades.

Measurements of the structure function scaling violations are most sensitive to the relative calibration of the muon and hadron energies; a 1% relative change can induce a 50 MeV error in $\Lambda_{\overline{MS}}$. This relative calibration has been determined by forcing E_{VIS} ($= E_{HAD} + E_\mu$) to be independent of $y = E_{HAD}/E_{VIS}$ after Monte Carlo corrections

for acceptance. The necessary corrections to E_μ (E_{HAD}) are .995 (1.007), well within the above absolute calibration errors.

The neutrino flux determination is broken into two parts. First, the absolute flux is found from the observed events and the world average measured total cross-section, $\sigma^{\nu N} = 0.676 \pm 0.014 \times 10^{-38} \text{ cm}^2 E_\nu (\text{GeV})$. Next, the relative flux at different energies for both ν_μ and $\bar{\nu}_\mu$'s is determined from the subset of events with low hadron energy, $E_{HAD} < 20 \text{ GeV}$. (The cross-section for these events is, up to small corrections, independent of energy and the same for both ν_μ and $\bar{\nu}_\mu$ as shown in Ref. 3) This technique is statistically limited and introduces an error less than 1% for the relative flux determination.

3. Structure Function Extraction

For the structure function extraction, additional cuts were imposed ($Q^2 > 1 \text{ GeV}^2$ and $E_\nu > 50 \text{ GeV}$) and the data were separated into twelve x bins from .015 to .850 and sixteen Q^2 bins from 1 to 600 GeV^2 . Integrating the differential cross-section (See section 1.) times flux over each (x, Q^2) bin yields two equations for the number of ν_μ ($\bar{\nu}_\mu$) events in terms of the two structure functions F_2 and xF_3 . The observed numbers of events are corrected by Monte Carlo techniques for acceptance and resolution smearing.

To solve the two equations, we assume a parameterization of R determined from SLAC measurements⁴ and apply isoscaler corrections for the 6.85% excess of neutrons over protons in iron. Based on our measurements⁵ of dimuon production, we include scattering off strange sea quarks and a slow-rescaling threshold suppression for the production of charm quarks. Radiative corrections⁶ are applied, and the cross-section is corrected for the massive W-boson propagator.

4. $xF_3(x, Q^2)$ Results

The xF_3 or valence structure function is predicted to have a simple QCD evolution independent of R and gluons. To leading order, xF_3 is expected to evolve as:

$$\frac{dx F_3(x, Q^2)}{d \ln Q^2} = \frac{\alpha_s(Q^2)}{\pi} \int_x^1 P_{qq}(z) x F_3\left(\frac{x}{z}, Q^2\right) \frac{dz}{z} \quad \text{or} \quad \frac{d \ln x F_3}{d \ln Q^2} \approx \alpha_s(Q^2) \Psi(x, Q^2)$$

where $\Psi(x, Q^2)$ is weakly dependent on the assumed form of $x F_3(x, Q^2)$ and has a well determined zero point.

As shown in Fig. 1a), our new results agree well with the predicted QCD scaling violations obtained from a next-to-leading order fit⁷ to the data with good agreement in the zero crossing point and the variation with x . This is in contrast to the results of the CDHSW group⁸ which show a significant disagreement with the QCD prediction. (The CDHSW group has attributed these disagreements to systematic errors that are strongly correlated between neighboring points; such errors do not seem to be present in the new CCFR data.) For $x > .5$, our measured results are consistent with $\bar{q} = 2xF_1 - xF_3$ being zero, indicating that F_2 can be substituted for xF_3 . With this substitution,

$\Lambda_{\overline{MS}}$ can be determined with an error ≈ 45 MeV. (We are not quoting a value for $\Lambda_{\overline{MS}}$ at this time but will do so in the next few months after the final systematic error estimates and studies are completed.)

5. $F_2(x, Q^2)$ Results

The F_2 structure function is accessible both through charged lepton and neutrino scattering. The lepton and neutrino structure functions are related by the "mean square charge" relationship:

$$\frac{F_2^{lN}}{F_2^{\nu N}} = \frac{5}{18} \left(1 - \frac{3s + \bar{s}}{5q + \bar{q}} \right)$$

The new CCFR results span the Q^2 range from the low energy SLAC⁹ (eD) results through the range covered by the BCDMS¹⁰ (μ D), EMC¹¹ (μ Fe) and CDHSW⁸ (ν Fe) measurements. (The deuterium data has been corrected to iron using the F_2^{eFe}/F_2^{eD} ratio measured at SLAC.¹²) The agreement, as shown in Fig. 2, between the CCFR, SLAC, and BCDMS data is quite good in both normalization (better than 2%) and shape. On the other hand, the CDHSW and EMC data differ substantially in the x region below .35, where the normalization is inconsistent by 10 to 20 %. The Q^2 dependence is also very different below 20 GeV² which will lead to differences in QCD constraints on the gluon distribution.

The predicted QCD evolution of F_2 is coupled to the gluon distribution, $G(x, Q^2)$, according to

$$\frac{dF_2(x, Q^2)}{d \ln Q^2} = \frac{\alpha_s(Q^2)}{\pi} \left[\int_x^1 F_2\left(\frac{x}{z}, Q^2\right) P_{qq}(z) dz + \int_x^1 G\left(\frac{x}{z}, Q^2\right) P_{qG}(z) dz \right].$$

In Fig.1b), we also display the slopes, $d \ln F_2 / d \ln Q^2$ for CCFR, BCDMS, and CDHSW along with a next-to-leading order fit to the CCFR data. The agreement of the CCFR data with the QCD predictions gives us confidence that a simultaneous fit of F_2 and xF_3 will allow a delineation of the gluon distribution.

This research was funded by the United States Department of Energy and the National Science Foundation.

References

1. W.K.Sakumoto *et al.*, *Nucl.Inst.Meth.*, **A294**, (1990) 179.
2. B.J.King *et al.*, *Nucl.Inst.Meth.*, **A302**, (1991) 254.
3. P.Auchincloss *et al.*, *Z.Phys.* **C48**, (1990) 411.
4. S.Dasu *et al.*, *Phys. Rev. Lett.* **61**, (1988) 1061.
5. M. Shaevitz, *Nucl. Phys. B. (Proc. Suppl.)* **19** (1991) 270.
6. A.De Rujula *et al.*, *Nucl. Phys.*, **B154**, (1979) 394.
7. A.Devoto *et al.*, *Phys. Rev.*, **D27**, (1983) 508.
8. P.Berge *et al.*, *Z.Phys.* **C49**, (1991) 187.
9. L.Whitlow, Ph.D. Thesis, SLAC - Report - 357 (1990) .

10. A.C.Benvenuti *et al.*, *Phys. Lett.* **223B**, (1989) 485; **237B**, (1990) 592.
 11. J.J.Aubert *et al.*, *Nucl. Phys.* **B259** (1985) 189; **B293** (1987) 740.
 12. A.Bodek *et al.*, *Phys. Rev. Lett.* **50** (1983) 1431; **51** (1983) 534.

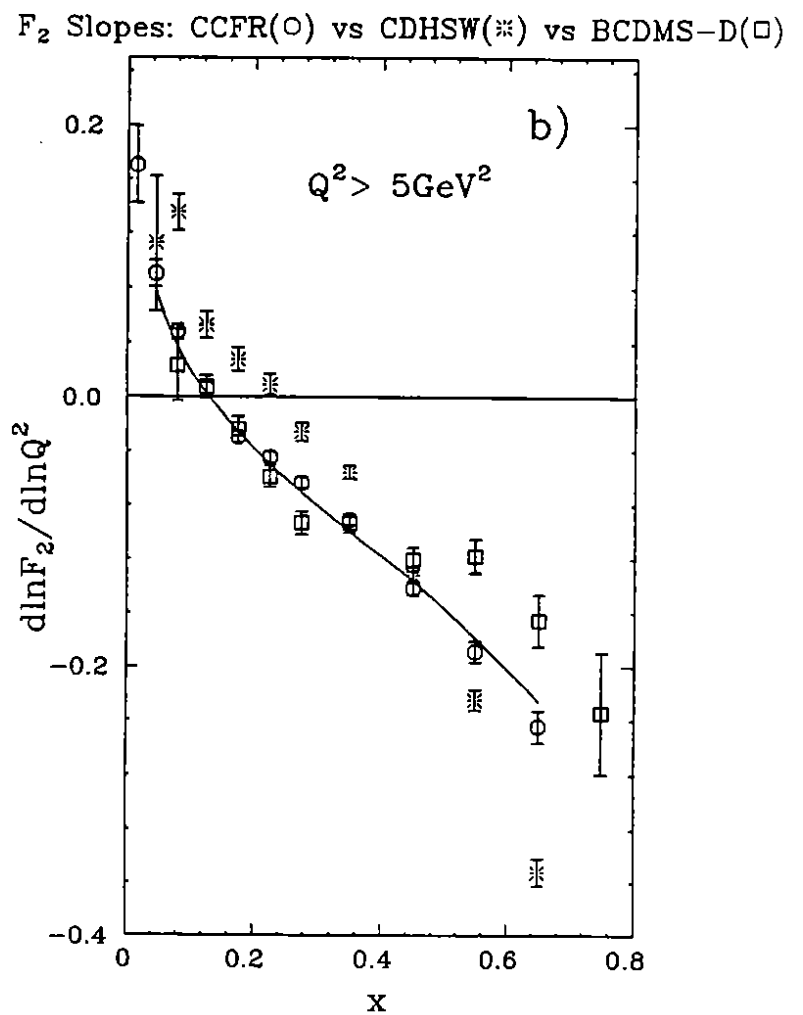
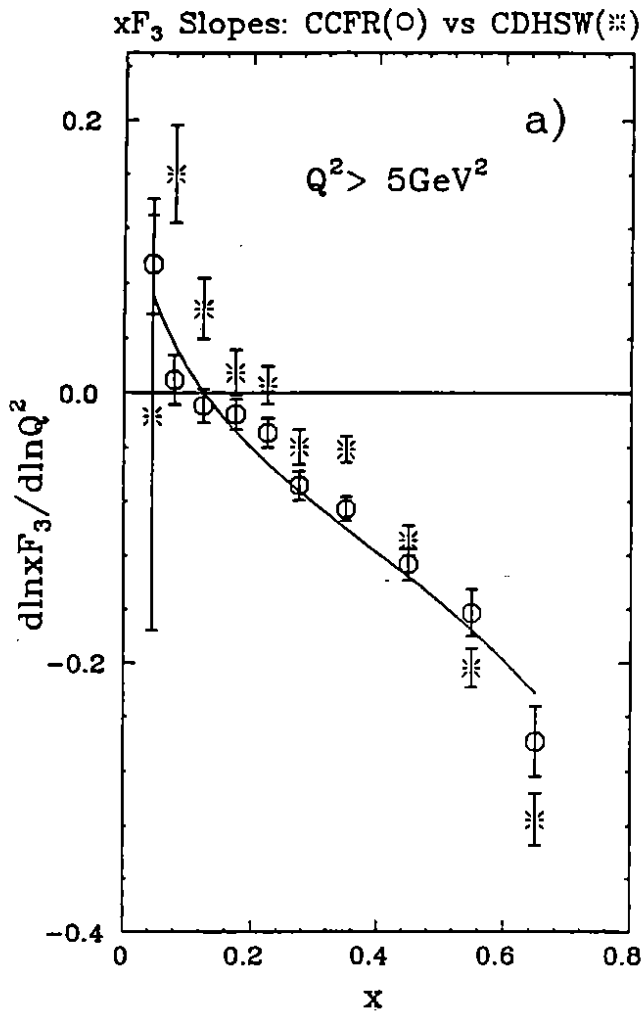


Fig. 1. Comparison of a) the $x F_3$ evolution for the CCFR and CDHSW measurements, b) the F_2 evolution for the CCFR, BCDMS, and CDHSW measurements.

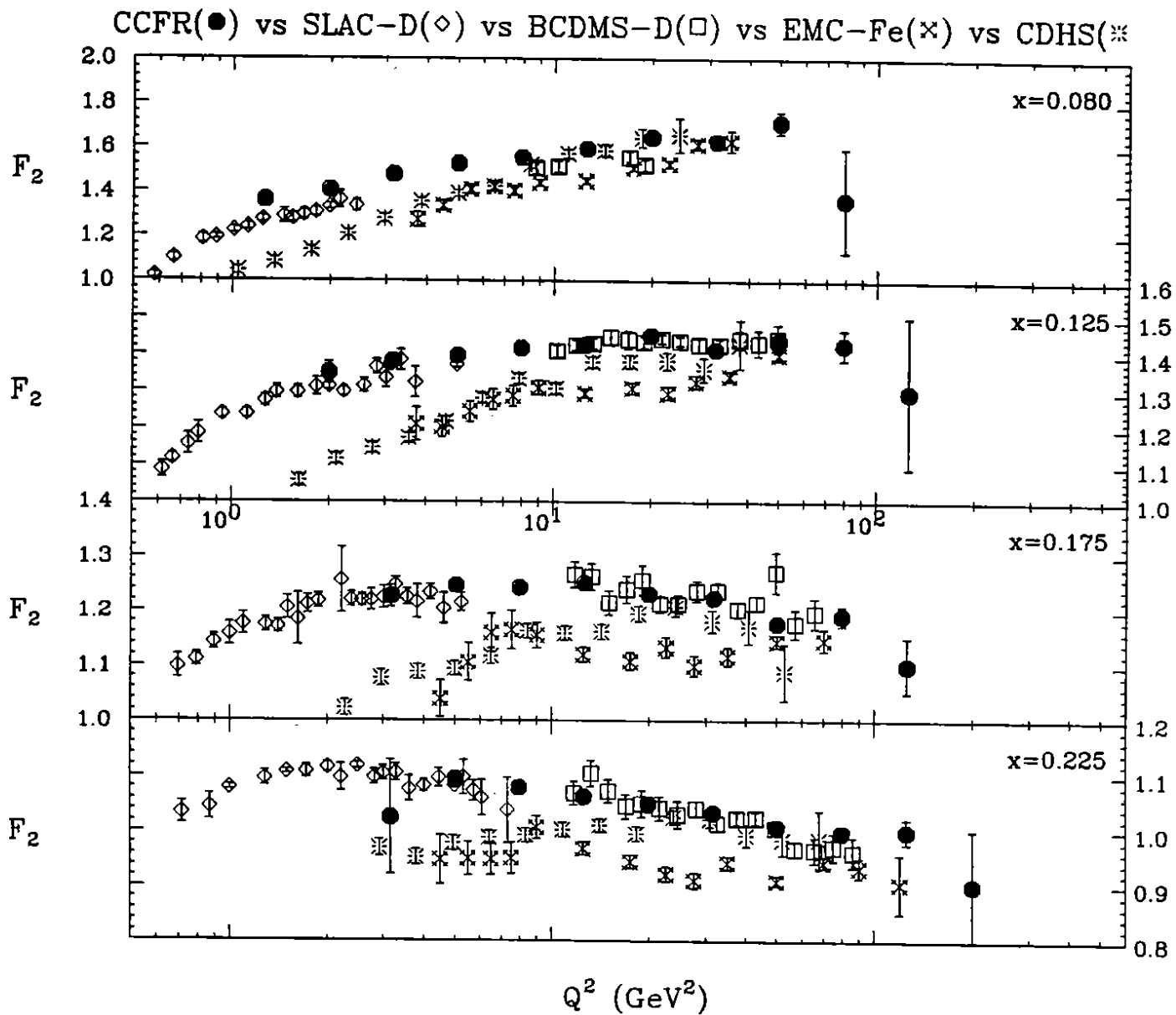


Fig. 2. Comparison of the measured F_2 structure function for the CCFR, SLAC, BCDMS, EMC, and CDHSW experiments for some representative low x bins.